Overcoming barriers for nitrate electrochemical reduction: By-passing water hardness

Aksana Atrashkevich, Ana Sofia Fajardo, Paul Westerhoff, W. Shane Walker, Carlos M Sánchez-Sánchez, Sergi Garcia-Segura

Overcoming barriers for nitrate electrochemical reduction: by-passing water hardness

Aksana Atrashkevich[a], Ana S. Fajardo[a,b,*], Paul Westerhoff[a], W. Shane Walker[a,c], Carlos M. Sánchez-Sánchez[b], Sergi Garcia-Segura[a,**]

[a]Nanosystems Engineering Research Center for Nanotechnology-Enabled Water Treatment, School of Sustainable Engineering and the Built Environment, Arizona State University, Tempe, AZ 85287-3005, USA

[b]Sorbonne Université, CNRS, Laboratoire Interfaces et Systèmes Electrochimiques (LISE), 4 place Jussieu, F-75005, Paris, France

[c]Civil Engineering, Center for Inland Desalination Systems, University of Texas at El Paso, El Paso, TX, USA

Article submitted to be published in Water Research

Corresponding author:

*e-mail: adossan3@asu.edu (Dr. Ana Sofia Fajardo)

**e-mail: Sergio.garcia.segura@asu.edu (Dr. Sergi Garcia-Segura)

Abstract

Water matrix composition impacts water treatment performance. However, matrix composition impacts have rarely been studied for electrochemical water treatment processes, and the correlation between the composition and the treatment efficiency is lacking. This work evaluated the electrochemical reduction of nitrate (ERN) using different complex water matrices: groundwater, brackish water, and reverse osmosis (RO) concentrate/brine. The ERN was conducted using a tin (Sn) cathode because of the high selectivity towards nitrogen evolution reported for Sn electrocatalysts. The co-existence of calcium (Ca^{2+}), magnesium (Mg^{2+}), and carbonate (CO_3^{2-}) ions in water caused a 4-fold decrease in the nitrate conversion into innocuous nitrogen gas due to inorganic scaling formation on the cathode surface. XRF and XRD analysis of fouled catalyst surfaces detected brucite ($Mg(OH)_2$), calcite ($CaCO_3$), and dolomite ($CaMg(CO_3)_2$) mineral scales formed on the cathode surface. Surface scaling created a physical barrier on the electrode that decreased the ERN efficiency. Identifying these main sources of ERN inhibition was a key to devising potential fouling mitigation strategies. For this reason, the chemical softening pre-treatment of a real brackish water was conducted and this significantly increased nitrate conversion and faradaic efficiency during subsequent ERN treatment, leading to a lower electric energy consumption per order. Understanding the ionic foulant composition responsible for influencing electrochemically-driven technologies are the first steps that must be taken to move towards niche applications such as decentralized ERN. Thus, we propose either direct ERN implementation in regions facing high nitrate levels in soft waters, or a hybrid softening/nitrate removal system for those regions where high nitrate and high-water hardness appear simultaneously.

Keywords: Electrochemical water treatment; Electrocatalysis; Nitrate reduction; Water hardness; Scaling; brackish waters

1. Introduction

Electrochemically-driven technologies for water treatment are emerging as competitive solutions for centralized and decentralized treatment given their high adaptability, compact reactor designs, and the possibilities of transforming pollutants into products of added value (Chaplin, 2019; Martínez-Huitle et al., 2015). The high relevance that electrified water purification will have in the near future is undeniable. Electrochemical processes can achieve effective removal of organics through electrochemical advanced oxidation processes (dos Santos et al., 2021; Moreira et al., 2017; Villanueva-Rodríguez et al., 2012), inactivation of pathogens through electrodisinfection (Garcia-Segura et al., 2021; Martínez-Huitle and Brillas, 2021), and even abatement of oxyanions such as nitrate by electrochemical advanced reduction processes (Sergi Garcia-Segura et al., 2018; van Langevelde et al., 2021).

Nitrate is one of the top ten water pollutants that commonly violate water quality regulations worldwide (Allaire et al., 2018; Rupert, 2008). The dramatic increase in nitrate concentration in water sources mainly located in rural areas is related to the extensive use of fertilizers in agriculture due to growing anthropogenic activities (Li et al., 2021). The World Health Organization (WHO) has set a maximum concentration level (MCL) of 10 mg NO_3^- defined in terms of mass of N per liter (NO_3—N L^{-1}) given the hazardous effects of nitrate for drinking water (WHO, 2016). Exposure to higher concentrations of nitrate above the suggested MCL has been associated to adverse respiratory effects (i.e., methemoglobinemia), thyroid problems, and cancer (Temkin et al., 2019; Torres et al., 2020). Water sources that violate the quality standards because of high nitrate levels result in the shutdown of water wells, limiting access to clean water, causing additional stressors for vulnerable populations.

Conventional treatment of nitrate polluted water requires in most cases the implementation of physical separation technologies (*i.e.*, ionic exchange, reverse osmosis) that generate undesired nitrate-rich brines (Amma and Ashraf, 2020; Liu et al., 2021). Other alternatives consider delicate biologic anammox treatment that requires specialized management and has a large physical footprint, both factors limiting widespread utilization in decentralized settings (Abdelfattah et al., 2020; Crittenden et al., 2012). Electrocatalytic reduction of nitrate (ERN) appears as a feasible solution given promising results reported

in literature on the study of synthetic solutions of nitrate (van Langevelde et al., 2021; Werth et al., 2021). Most research in these works have focused on the discovery of electrocatalytic materials that overcome sluggish nitrate reduction kinetics as well as control product selectivity in matrix-free solutions (Lim et al., 2021; Sanjuán et al., 2020; Y. Zhang et al., 2021). Very few examples addressing the impact on ERN performance of a complex matrix such as the one present in nuclear (Katsounaros et al., 2009) and textile (Su et al., 2017) wastewater effluents can be found in the literature.

The ERN mechanism for producing either ammonia (NH_3) or nitrogen gas (N_2) presents a common initial reduction step, the reduction of nitrate to produce nitrite (NO_2^-), which thereafter separates in two independent reaction pathways leading to each final product (i.e., NH_3 and/or N_2). Nitrate reduction towards ammonia following Reaction (1) can be a resourceful approach for sustainable nitrogen recovery for agriculture applications (Gabriel Antonio Cerrón-Calle et al., 2022; Katsounaros, 2021; van Langevelde et al., 2021). The nitrate reduction towards innocuous nitrogen gas by Reaction (2) is of utmost importance for drinking water purposes (Flores et al., 2022).

$$NO_3^- + 9H_2O + 8e^- \rightarrow NH_3 + 9OH^- \quad (1)$$

$$2NO_3^- + 12H_2O + 10e^- \rightarrow N_2 + 12OH^- \quad (2)$$

Because of concerns regarding availability, cost, and supply chains associated with platinum group metals (PGMs) or rare earth elements, significant advances are being conducted to develop competitive electrocatalysts based on earth-abundant materials such as tin (Sn), copper (Cu), and cobalt (Co) (G.A. Cerrón-Calle et al., 2022b; Fajardo et al., 2021; Katsounaros, 2021; X. Zhang et al., 2021). High competitiveness of Sn electrodes that enable fast nitrate reduction kinetics with a very high selectivity towards N_2 has been demonstrated (Ambrosioni et al., 2014; Fajardo et al., 2021; Katsounaros et al., 2012; Tada and Shimazu, 2005). Understanding interfacial effects that may condition the long-term sustained performance of this electrodes it is relevant to advance technology readiness level of competitive ERN systems. However, the promising results of ERN electrocatalysts have been at fundamental level while exploring performance of the systems in ultrapure solutions and not in real water matrices polluted with nitrate such as groundwater, brackish waters, brines, wastewaters, and others (Garcia-Segura et al., 2020a).

Co-existence of different ions may be detrimental for sustained long-performance of these promising electrocatalytic materials. Co-existing species may compete with the target pollutant causing a decrease in treatment efficiency or decrease the operational life of the electrode as result of material aging, fouling, and/or scaling. Besides water composition, the pH is one of the most critical water quality parameters when considering water use for drinking purpose. The speciation of many compounds depends on the solution pH. Water distribution systems aim to maintain pH near to circumneutral conditions to avoid pipe corrosion but also to ensure potable characteristics when reaching the end user. It is generally reported that ERN treatment results in an increase of water pH given the reduction of nitrate according to Reactions (1) and (2). Most works in literature conduct electrolysis in pure water matrices without controlling pH, which reaches values close to 9–11 (Fajardo et al., 2021; Nobial et al., 2007). Water treatment should ideally provide clean water with a pH ranging from 6-9, which may be ensured by the presence of pre-existing buffers in solution (i.e., carbonate system) or other pH controlling techniques. Therefore, understanding the major influential factors on the ERN are essential to develop preemptive strategies that enable successful technology transfer into challenging real conditions.

Groundwater is especially impacted with high nitrate concentrations in regions of high agricultural activity. Nevertheless, groundwater of non-agricultural regions may be polluted with nitrate over MCL, but considered as a nitrate-poor water source (*e.g.*, nitrate below 30 mg NO_3-N L^{-1}). A possible solution already suggested in the literature is to concentrate the nitrate and all other ions in solution prior to ERN using separation technologies such as reverse osmosis, ionic exchange, or capacitive deionization (van Langevelde et al., 2021; Werth et al., 2021; Yang et al., 2013). This pre-concentration approach will produce electrolyte compositions close to the ones displayed by either brackish or brine streams. For this reason, real water samples from brackish and brine streams are studied herein, besides synthetic water. The amount of nitrate added as contaminant in all three types of water source studied has been kept constant (30 mg NO_3-N L^{-1}) in order to reach a fair comparison. Treatment of groundwater with either decentralized or centralized electrochemically-driven technologies can be a suitable solution for purification of waters with nitrate content over MCL. However, groundwater, brackish, and brine have complex water matrices

that were barely explored in literature while studying the electrochemical treatment. The effect of co-existing electrolytes during ERN should be addressed (Sergi Garcia-Segura et al., 2018; Katsounaros and Kyriacou, 2008). Understanding the impact of ionic species of environmental relevance is an urgent need to assess the competitiveness of emerging technologies under real conditions (Flores et al., 2022; Werth et al., 2021).

This work aims to elucidate common anions/cations in real water matrices which might become a barrier to the efficient ERN. Especial attention is driven to understand scaling induced by water hardness ions, as the generation of physical barrier demonstrated to deleteriously affect performance of ERN. The effect of complex water matrices is assessed exploring the treatment of realistic multiple ion solute samples of ground, brackish, and brine waters. These water sources with elevated nitrate level have been identified as possible niche applications for decentralized electrified technologies (Hansen et al., 2017; Maxwell et al., 2020). The research showed which water matrices may benefit from implementing pre-treatment systems prior to electrochemical nitrate reduction. Therefore, feasible alternatives to overcome challenges associated to specific species are proposed and evaluated. In particular, chemical softening of brackish water prior to the ERN treatment was conducted. Implementation of management strategies should be considered when exploring real world treatment scenarios.

2. Materials and methods

2.1 Chemicals and solutions

Sodium nitrate ($NaNO_3$), calcium sulfate dihydrate ($CaSO_4 \cdot 2H_2O$), magnesium sulfate heptahydrate ($MgSO_4 \cdot 7H_2O$), sodium bicarbonate ($NaHCO_3$), sodium chloride (NaCl), sodium phosphate monobasic monohydrate ($NaH_2PO_4 \cdot H_2O$), sodium fluoride (NaF), and sodium metasilicate nonahydrate ($Na_2SiO_3 \cdot 9H_2O$) compounds, with purity > 99%, were purchased from Sigma-Aldrich to evaluate single component effects as well as to verify their interaction together by mimicking groundwater matrices. Sulfuric acid (H_2SO_4 96%, Sigma Aldrich) and sodium hydroxide (NaOH 99%, Sigma Aldrich) solutions were used to adjust the pH when required. Table 1 summarizes the analytical characterization of the

different water matrices treated by the ERN. Synthetic aqueous solutions containing 30 mg NO_3^--N L^{-1} (133 mg NO_3^- L^{-1}) were prepared with distilled water (pH = 5.8 ± 0.1; conductivity 10 ± 5 μS cm^{-1}) and they correspond to entries from A to I in Table 1. This nitrate concentration was selected since it is within the common ranges found in groundwaters (WHO, 2016). Sodium sulphate (Na_2SO_4, > 99% purity, Sigma-Aldrich) was used as a supporting electrolyte; the "Blank" (or control) matrix listed in Entry A is a brackish ternary solution containing 25 meq L^{-1} of sodium sulfate and 2.14 meq L^{-1} of sodium nitrate. Entry B is a complex synthetic brackish water prepared according to the NSF-challenge water recipe from the National Sanitation Foundation (NSF International) which is a model for natural groundwater and has already been applied in many other studies (Gröhlich et al., 2017; Usman et al., 2018). The groundwater recipe emulates the real representative concentrations of electrolytes found in environmental samples. Thus, the effect of coexisting ions was explored using the meaningful concentration of each species as reported for the composition of Entry B but considering only single solute compositions. In Table 1, Entries C through I are brackish quaternary solutions that include the constituency of Entry A with the addition of a single cation, anion, or silica; the concentration of each of these constituents was selected in basis of the general compositions reported for groundwaters (defined by Entry B). Entries J and L correspond to real brackish groundwater and reverse osmosis (RO) concentrate/brine water collected in Texas (USA), respectively, where a constant amount of nitrate pollutant (30 mg NO_3^--N L^{-1}) is added.

Table 1. Characterization of the brackish water matrices tested in this work (all prepared with 30 mg NO_3^--N L^{-1}).

Entry	Water matrices	Initial pH	Conductivity (mS cm^{-1})	Cations (mg L^{-1})				Anions (mg L^{-1})						Silica (mg SiO_2 L^{-1})
				Ca^{2+}	Mg^{2+}	Na^+	K^+	NO_3^-	HCO_3^-	Cl^-	F^-	PO_4^{3-}	SO_4^{2-}	
A	Blank	5.95	3.1	-	-	625	-	133	-	-	-	-	1201	-
B	Synthetic Brackish Groundwater	6.22	3.85	41	12	749	-	133	183	72	1	0.12	1347	20
C	Ca^{2+}	5.95	3.1	41	-	625	-	133	-	-	-	-	1299	-
D	Mg^{2+}	5.95	3.1	-	12	625	-	133	-	-	-	-	1249	-
E	Si_2O	5.95	3.1	-	-	632	-	133	-	-	-	-	1201	20
F	HCO_3^-	5.95	3.1	-	-	693	-	133	183	-	-	-	1201	-
G	Cl^-	5.95	3.1	-	-	671	-	133	-	72	-	-	1201	-
H	F^-	5.95	3.1	-	-	626	-	133	-	-	1	-	1201	-
I	PO_4^{3-}	5.95	3.1	-	-	625	-	133	-	-	-	0.12	1201	-
J	Real Brackish Groundwater*	7.90	4.5	130	30	725	13	133	99	1352	1	n.m.	269	n.m.
L	Real RO Brine*	8.10	20	567	157	3268	74	133	417	5522	4	n.m.	1218	n.m.

* Identification and quantification of water composition was conducted by ionic chromatography. "n.m." – not measured.

2.2 Electrochemical experiments

The electrochemical reduction of nitrate was conducted under galvanostatic operating mode applying a constant current intensity of 120 mA (i.e., current density j = 40 mA cm^{-2}) using a power supply TENMA 72-2710. The undivided electrochemical glass batch cell was equipped with a tin cathode plate (Sn, 99.99% purity from McMaster-Carr/USA). Electrodes of Sn have shown excellent electrocatalytic activity for ERN with outstanding selectivity towards N_2 (Dortsiou et al., 2013; Fajardo et al., 2021). The electrochemical cell was completed with a DSA® Ti/IrO_2 (DeNora/USA) mesh anode. Both electrodes had a geometric area of 3 cm^2 delimited with Teflon tape and were located with a 1.0 cm electrode gap distance within the electrochemical cell. Solutions of 100 mL were treated under magnetic stirring at 550 rev min^{-1} to ensure transport of electroactive species towards/from the electrode. Samples were withdrawn over time and analyzed for aqueous nitrogen species, conductivity, and pH. Experiments were performed in triplicate, and deviations between them were lower than 5% for all trials. Statistical paired t-test analysis was conducted for experimental results using Minitab® statistical software considering an $\alpha = 0.05$. Experiments conducted while maintaining constant the pH ($5.5 < pH < 6.4$), small quantities of 0.1 M

H_2SO_4 (< 3 μL) were gradually added every 7-8 min during the 360 min of reaction. For the case of carbonate buffer, pure CO_2 gas was bubbled in the solution during the experiment. Statistically significant difference between experiments was evaluated based on *p*-value.

2.3 Analytical techniques

The pH and conductivity were measured with a Thermo Scientific Orion Star A221 pH-meter and an A322 conductivity meter, respectively. The concentrations of NO_3^--N, NO_2^--N and NH_3-N species were quantified using the HACH kits TNT 835, TNT 839 and TNT 830, respectively, by an HACH DR 6000 UV-vis spectrophotometer. From experimental quantification of nitrate concentration over electrolysis time the nitrate conversion was calculated according to Equation (3). The selectivity (S_x) of nitrogen gas was estimated from Equation (4).

$$Nitrate\ conversion\ (\%) = \frac{C_{nitrate,i} - C_{nitrate,t}}{C_{nitrate,i}} \times 100\% \quad (3)$$

$$S_{N_{gas}}\ (\%) = \frac{C_{N_2,t}}{C_{nitrate,i} - C_{nitrate,t}} \times 100\% \quad (4)$$

where $C_{nitrate,i}$ is the nitrate concentration at the beginning of the treatment (t = 0 min) in mg NO_3^--N L^{-1}, and $C_{nitrate,t}$ is the nitrate concentration at time *t* in mg NO_3^--N L^{-1}, and $C_{N_2,t}$ is the concentration of a nitrogen gas in mg $N_2 - N\ L^{-1}$ at time *t*.

The efficient use of electrons delivered to promote nitrate reduction was evaluated in terms of Faradaic efficiency (FE) as defined by Equation (5). The FE is an electrocatalytic figure of merit that defines the number of electrons consumed for nitrogen gas evolution reaction relatively to the total charge delivered according to Faraday's law. The FE shows the effectiveness of the actual charge transfer during the reaction of interest.

$$FE(\%) = \frac{Q_{reaction}}{Q_{total}} \times 100\% = \frac{n\ F\ N_i}{3600\ I\ t} \times 100\% \quad (5)$$

where $Q_{reaction}$ is the empirical charge consumed in the reaction of interest (C), Q_{total} is the total charge consumed during electrochemical process (C), *n* is the amount of electrons required per mole of product

(10 mol e^-/mol N_2), F is the Faraday constant (96 487 C eq^{-1}), N_i is the amount of product generated during the electrolysis (mol N_2), I is the applied current intensity (A), t is the time (h), 3600 is a unit conversion factor (s h^{-1}). To evaluate the energy requirements of ERN, the engineering figure of merit electric energy per order (*EE/O*) was computed according to Equation (6) (Bolton et al., 2001; Marcos-Hernández et al., 2022).

$$EE/O(kWh\ m^{-3}\ order^{-1}) = \frac{E_{cell}\ I\ t}{V_s\ log\left(\frac{C_{nitrate,i}}{C_{nitrate,t}}\right)} \quad (6)$$

where E_{cell} is the average of the cell potential (V) and V_s is the volume of the treated solution (L). Assuming that the electrochemical reduction of nitrate in the experiments follows a *pseudo*-first order kinetics (Equation (7)) the *EE/O* can be simplified as Equation (8).

$$log\left(\frac{C_{nitrate,i}}{C_{nitrate,t}}\right) = 0.4343k_1t \quad (7)$$

$$\text{EE/O}\ (kWh\ m^{-3}\ order^{-1}) = \frac{6.39\ \ 10^{-4}E_{cell}\ I}{V_s\ k_1} \quad (8)$$

where, k_1 is the *pseudo*-first order kinetics constant (s^{-1}).

The concentrations of inorganic ions present in the real brackish and RO brine waters were quantified with a Thermo Scientific simultaneous cation and anion ion chromatography (IC) system. Cation concentrations were analyzed with a DIONEX Aquion with an IonPac CS16 (5x250 mm) column, a 10 µL sample injection volume, and 47 mmol L^{-1} methanesulfonic acid (MSA) as eluent with an eluent flow rate of 1 mL min^{-1}. Anions were analyzed with a DIONEX Integrion HPIC with an IonPac AS18-Fast-4µm column, a 10 µL sample injection volume, 30 mmol L^{-1} of potassium hydroxide as eluent, and an eluent flow rate of 1 mL min^{-1}.

Chemical precipitation is one of the more common methods used to soften water (Chao and Westerhoff, 2002). The lime-soda softening method was used to decrease water hardness of brackish water prior ERN treatment. The chemicals used were lime (calcium hydroxide, $Ca(OH)_2$) and soda ash (sodium carbonate, Na_2CO_3). Lime was applied to remove chemicals that cause carbonate hardness, while soda ash was used to remove chemicals that cause non-carbonate hardness. When lime and soda ash were added,

hardness-causing species formed insoluble precipitates such as calcium carbonate ($CaCO_3$) and magnesium hydroxide ($Mg(OH)_2$). Solid-liquid separation was performed to recover the liquid sample first by gravity separation and after trough filtration using 0.45 μm filter.

Analysis of the surface of the cathode included its elemental composition, determined by x-ray fluorescence (XRF) using a Thermo Scientific PTS22163. Electrodes were gently rinsed with ultrapure water to ensure that measurements corresponded to scaled solid deposited on the surface of the electrode during water treatment and not result of electrolyte evaporation. The crystalline structure of collected solids deposited on the electrode surface was analyzed by the X-ray diffraction (XRD) using a PANalytical AERIS X-ray diffractometer within 2θ range from 10° to 100° with a step of 0.01°.

3. Results and discussion

3.1 Effect of pH control on the electrochemical reduction of nitrate

The effect of nearly constant bulk water pH conditions on treatment performance was explored to evaluate the impact in nitrate conversion and product selectivity. Figure 1 shows that the ERN during the treatment of 30 mg NO_3^--N L^{-1} using Sn electrode attained predominantly electrocatalytic selectivity towards N_2. The high product selectivity towards innocuous N_2 (ca. 70%) is one of the most promising characteristics of Sn as an electrode material for the ERN and is explained by the intrinsic electrocatalytic properties of the electrode. During the blank experiments conducted using an unbuffered solution, the nitrate conversion achieved 82% and nitrate concentration diminished to 5.5 mg NO_3^--N L^{-1}, which is below the MCL level of 10 mg NO_3^--N L^{-1}. The pH of unbuffered solution increased from 5.95 up to 10.15, which is a commonly observed feature in many other studies, regardless of electrode materials (Fuladpanjeh Hojaghan et al., 2019; Szpyrkowicz et al., 2006). The pH increase is explained by the release of hydroxyl anions during reduction processes described in Reaction (1) and (2). During electrochemical processes, the generation of OH^- ions is promoted on the surface of the cathodes, causing the solution pH to increase over time. The results of unbuffered pH were used to benchmark the performance of pH-controlled systems through: (i) CO_2 bubbling, and (ii) active pH control through acid addition (i.e., H_2SO_4).

The pH control by carbonate buffer through CO_2 bubbling is a common practice at water treatment plants to lower water pH, especially after softening processes. Note that CO_2 is an acid gas that when dissolved in water forms carbonic acid (Cerrón-Calle et al., 2022a). Here CO_2 bubbling was employed to control solution pH during ERN. The CO_3^{2-} concentration was controlled through the gas-liquid equilibria in an open system. Statistical paired *t*-test analysis showed similar nitrate removal values for the blank and CO_2 bubbling experiments (ca. 70%) without statistically significant difference based on obtained *p*-value of 0.208. Moreover, the selectivity towards N_2 (ca. 64%) remained the same with high reproducibility (*p*-value = 0.166). These results suggest that a possible small content of dissolved oxygen within the electrochemical cell was not significant to inhibit nor compete with the nitrate reduction Reactions (1) and

(2). Therefore, ERN treatment may be conducted in principle under unbuffered conditions without detriment on performance in the pH range between 6 and 11.

Acidification by adding liquid reactants instead of a gas is an alternative approach to control pH changes during treatment. Sulfuric acid is the most common strong acid used at water treatment plants to lower pH, usually ahead of coagulation or membrane processes. Additionally, sulfuric acid was selected given the inert character of sulfate anions as electrolytes in electrochemical systems. The initial pH of 5.95 was maintained during the ERN treatment of 30 mg NO_3^--N L^{-1} nitrate solution. The experiments with continuous acidification led to nitrate conversion of 80% which is not significantly different neither from blank (*p*-value = 0.500) nor from buffered experiment with CO_2 (*p*-value of 0.152). The results in Fig. 1 allowed to infer negligible impact of pH control on the overall reduction kinetics as well as the final product selectivity. Considering these outcomes, ERN treatment can be conducted without strict pH control but may require pH adjustment prior its use for drinking water applications. Following sections explore the treatment of natural water solutions without any pH adjustment given that this operational condition is the easiest scalable approach without additional costs associated to continuous pH control.

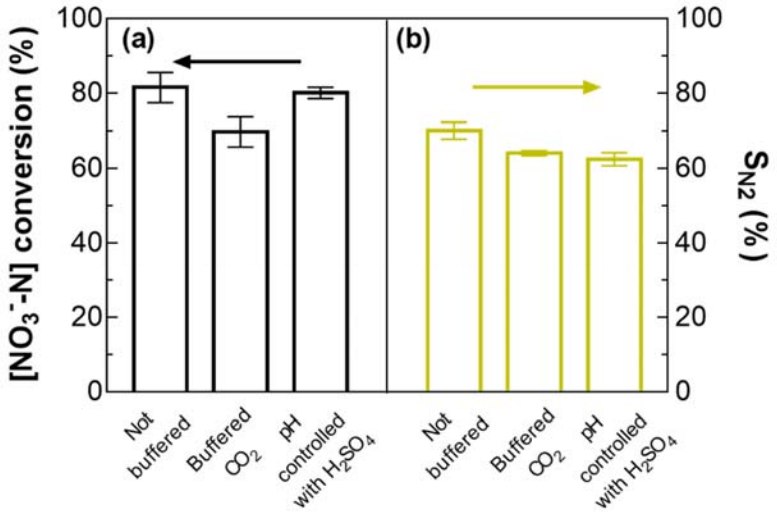

Figure 1. *Electrocatalytic reduction of 30 mg NO_3^--N L^{-1} in 12.5 mM Na_2SO_4 at 40 mA cm^{-2} after 360 min of treatment in unbuffered solution, carbonate buffer through CO_2 bubbling, pH-controlled solution by H_2SO_4 addition: a) nitrate conversion, and b) selectivity towards nitrogen gas.*

3.2 Effect of different inorganic ions on the electrochemical reduction of nitrate

Figure 2 illustrates a significant loss of ERN performance when comparing idealistic treatment conditions of nitrate in a simple ternary brackish water solution (entry A in Table 1) with a more complex synthetic brackish groundwater that contains a mixture of coexisting ionic species (entry B in Table 1). Figure 2a shows the common behavior reported for nitrate electrochemical reduction in which the sluggish reduction kinetics is controlled by the first charge transfer reaction as limiting step. The ERN treatment of 30 mg NO_3^-N L^{-1} in simple ternary water solution (Table 1 – entry A) exhibited a gradual decay during the first 360 min treatment time until reaching 5.5 mg NO_3^-N L^{-1} (below MCL), which corresponded to a nitrate conversion of 82%. This conversion fits well with a *pseudo*-first order constant (k_1) with the value $k_1 = 7.8 \times 10^{-5}$ s^{-1} ($R^2 = 99.8\%$). In contrast, the treatment of 30 mg NO_3^-N L^{-1} in the complex synthetic brackish groundwater (Figure 2b and Table 1 – entry B) decreases effective conversion 4-fold from 82% removal down to 19%, and decreases the rate 8-fold as observed from the *pseudo*-first order rate constant of 0.95×10^{-5} s^{-1} ($R^2 = 97.9\%$). The coexistence of other inorganic ions in the system clearly impacted the ERN performance. To elucidate which ions drive such significant decrease in the treatment performance, the individual effect of each ion was tested on the ERN using the same concentrations present in the groundwater sample.

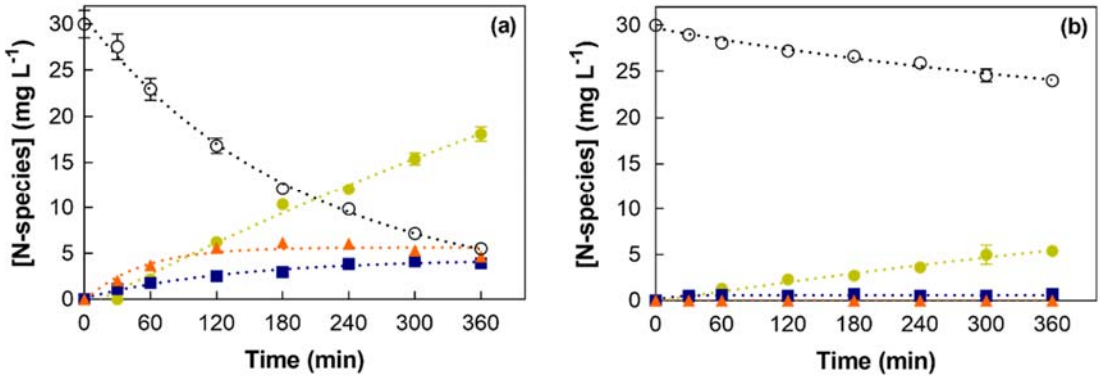

Figure 2. *Evolution of nitrogenated species, (○) NO_3^-N, (▲) NO_2^-N, (■) NH_3-N, (●) N_2-N, over time for the electrochemical reduction of groundwater at 40 mA cm^{-2} with (a) blank solution (entry A in Table 1): 30 mg NO_3^-N L^{-1} in 12.5 mM Na_2SO_4 (b) synthetic brackish solution (entry B in Table 1).*

Figure 3 summarizes the effect on nitrate conversion of single ionic species in solution assuming that Na^+ and SO_4^{2-} are inert electrolytes on nitrate conversions in the electrochemical systems (ions also present in the blank as supporting electrolyte). Anionic species commonly found in natural waters (PO_4^{3-}, HCO_3^-, F^- and Cl^-) had slight effects on the ERN performance where the nitrate conversion attained was statistically the same. The treatment attained desired residual concentrations of nitrate below recommended MCL after ERN treatment in all instances. Nitrate removal in presence of different anionic species has negligible effect because these species are not susceptible of being reduced under these operation conditions, which would explain the low impact on ERN. Dissolved silica (*e.g.*, $SiOH_4$; pK_a=10.4) is found in groundwaters between 5 to 50 mg SiO_2 L^{-1}, but its evaluation demonstrated negligible impact on ERN performance. The coexistence of these ionic species (PO_4^{3-}, HCO_3^-, F^- and Cl^-) does not seem to explain the drastic loss in performance observed on ERN in Figure 2b.

In contrast, divalent cations exert a stark impact on nitrate abatement. The presence of 0.5 mmol L^{-1} Mg^{2+} led to the lowest nitrate conversion with 26% with lower selectivity towards nitrogen gas. Meanwhile with dosed Ca^{2+}, the nitrate reduction achieved 74% conversion, which is close to the 82% observed for the water solution containing solely nitrate and electrolyte. Analysis of equilibrium speciation of the complex

313 synthetic brackish groundwater matrix (Table 1 Entry B) with Visual Minteq v3.1 revealed that 99.3% of
314 nitrate remains not complexed, so complexation does not explain the observed decrease in denitrification.
315 Electrochemically-driven nitrate reduction takes place at the cathode surface mediated by direct
316 charge transfer processes (Flores et al., 2022; S. Garcia-Segura et al., 2018). Electrocatalytic reactions are
317 heterogeneous in nature and require an intimate interaction between the electroactive target species (*i.e.*,
318 nitrate) and catalytic sites on the electrode surface. Electrode scaling induced by the precipitation of
319 insoluble species on the vicinity of the electrode surface may result in the inhibition of mass transport
320 from/towards electrodes. It is important to remark that cathodic surfaces become, locally, alkaline due to
321 proton consumption during ERN as stated in reactions (1) and (2), as well as during the competitive
322 hydrogen evolution Reaction (9).

$$2H_2O + 2e^- \rightarrow H_2 + 2OH^- \quad (9)$$

323 Interface studies report that the localized pH on the cathode surface reaches values ranging between
324 10-11, even when bulk water pH is measured as < 7 (Monteiro and Koper, 2021; Tlili et al., 2003). Figure 4a
325 illustrates the solubility diagram of Mg^{2+} and Ca^{2+} ions regarding their hydroxide insoluble salts in function
326 of the pH as defined by equilibrium Reactions (10) and (11) with thermodynamic solubility constants (K_{sp})
327 of $10^{-10.74}$ and $10^{-5.30}$ at 25 ºC, respectively (Snoeyink and Jenkins, 1980). Note that precipitation of $Ca(OH)_2$
328 is thermodynamically not feasible at given concentrations and localized pH condition of 10-11 at cathodic
329 surfaces given its higher solubility. Meanwhile, solubility of Mg^{2+} drastically decreases under alkaline pH
330 conditions with values as low as $10^{-2.74}$ M at pH 10 or $10^{-4.74}$ M at pH 11. Nucleation and growth of insoluble
331 $Mg(OH)_2$ on the electrode surface would explain the drastic decrease on performance since the scaling acts
332 as a physical barrier inhibiting the charge transfer process at the interface.

$$Mg(OH)_2 \leftrightharpoons Mg^{2+} + 2OH^- \; pK_{sp} = 10.74 \text{ at } 25\,^{\circ}C \quad (10)$$

$$Ca(OH)_2 \leftrightharpoons Ca^{2+} + 2OH^- \; pK_{sp} = 5.3 \text{ at } 25\,^{\circ}C \quad (11)$$

333 It is important to remark that solutions only containing Ca^{2+} ions would hardly precipitate at given
334 conditions, which therefore does not inhibit ERN treatment (see Figure 3a). These results would pinpoint a

driving effect of Mg^{2+} as major inhibitor for sustained ERN treatment. However, Ca^{2+} ions below pH 10.5 tend to precipitate not because the formation of insoluble $Ca(OH)_2$, but because of another much more insoluble species (*i.e.*, $CaCO_3$). Thus, the impact of Ca^{2+} on the ERN depends on alkalinity as the CO_3^{2-} availability in solution defines Ca^{2+} precipitation (Figure 4b).

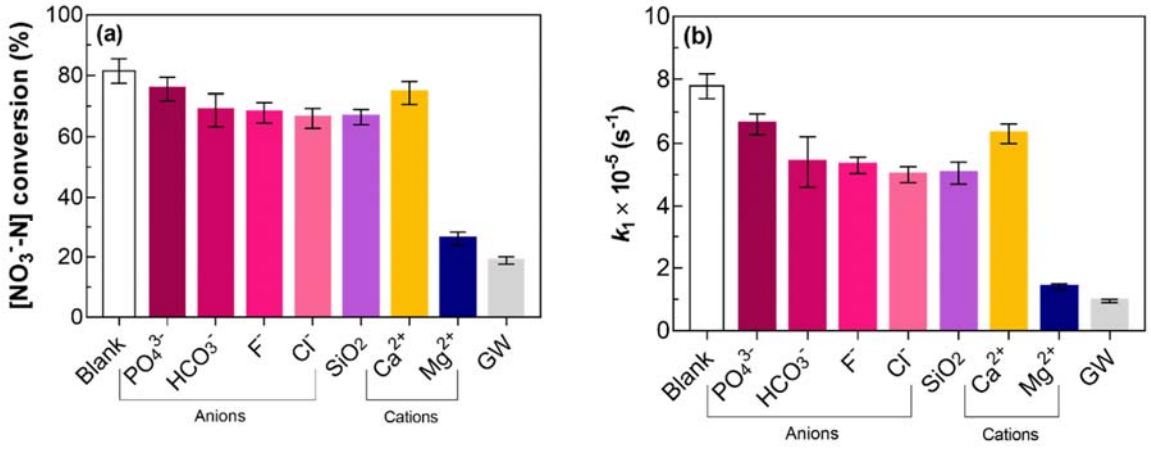

Figure 3. (a) *Nitrate conversion and (b) kinetic constants after 360 min of electrocatalytic treatment with Sn cathode at 40 mA* cm^{-2} *in different water matrices: ultrapure water, single competitive ionic species, or synthetic complex brackish groundwater matrix (GW). Composition of the matrices is summarized in Table 1.*

Note that carbonate species at the initial bulk solution pH is primarily bicarbonate ion (HCO_3^-), but the speciation close to the alkaline region on the cathode surface is likely carbonate ion (CO_3^{2-}) as indicated by the speciation diagram of Fig. 4c according to the acid-base equilibrium of Reaction (12) with characteristic pK_{a2} value of 10.3 (Lertratwattana et al., 2019; Snoeyink and Jenkins, 1980). The relative concentration of CO_3^{2-} and Ca^{2+} define the oversaturation conditions that may induce the precipitation of insoluble $CaCO_3$ as deduced from the solubility diagram of Figure 4b. Carbonate insoluble species are formed following Reactions (13) and (14) with K_{sp} of $10^{-8.34}$ and $10^{-5.30}$ at 25 ºC, respectively (Snoeyink and Jenkins, 1980). The high concentration of Ca^{2+} ions as the main hardness species in real brackish and brine

water would explain the identification of calcite as predominant scalant formed on the alkaline cathodic surface in entries J and L, respectively.

$$HCO_3^- \leftrightharpoons H^+ + CO_3^{2-} \quad pK_{a2} = 10.3 \text{ at } 25\ ^\circ C \tag{12}$$

$$CaCO_{3(s)} \leftrightharpoons Ca^{2+} + CO_3^{2-} \quad pK_{sp} = 8.34 \text{ at } 25\ ^\circ C \tag{13}$$

$$MgCO_{3(s)} \leftrightharpoons Mg^{2+} + CO_3^{2-} \quad pK_{sp} = 5.30 \text{ at } 25\ ^\circ C \tag{14}$$

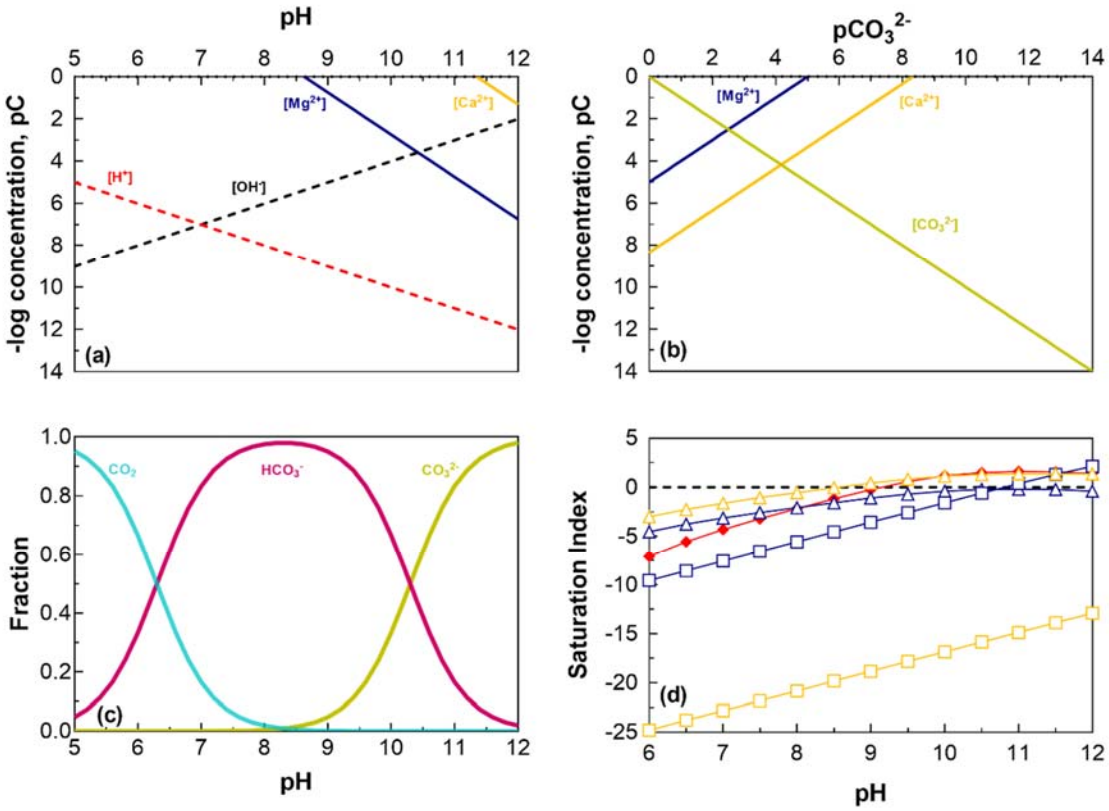

Figure 4. (a) *Solubility diagram of Mg^{2+} and Ca^{2+} in function of pH considering the formation of insoluble hydroxide precipitates $Mg(OH)_2$ and $Ca(OH)_2$.* ***(b)*** *Solubility diagram of Mg^{2+} and Ca^{2+} in function of CO_3^{2-} concentration.* ***(c)*** *Speciation of carbonate in function of pH.* ***(d)*** *Saturation index as a function of pH of $Ca(OH)_2$ (yellow □), $CaCO_3$ (yellow △), $Mg(OH)_2$ (blue □), $MgCO_3$ (blue △) and*

359 *$CaMg(CO_3)_2$ (red ◆) considering a molar ratio composition of Ca^{2+}:CO_3^{2-}:Mg^{2+} of 1:1:0.25 in a water*
360 *matrix at equilibrium for initial concentration of Ca^{2+} of 1 mM..*
361
362 To mimic scaling formation under experimental electrolyte composition during ERN, saturation
363 indexes of possible precipitated solids over pH were plotted in Figure 4d for an actual water matrix
364 (considering a molar ratio composition of Ca^{2+}:CO_3^{2-}:Mg^{2+} of 1:1:0.25 in a water matrix at equilibrium for
365 initial concentration of Ca^{2+} of 1 mM). The saturation index (SI) is defined as the logarithmic difference
366 between product ion activity (or activity quotient) and product solubility constant. The positive value of SI
367 illustrates that precipitation of the solids is thermodynamically favorable (supersaturated conditions), while
368 negative value of SI suggests undersaturated conditions. However, the rate of precipitation is controlled by
369 the kinetics of nucleation of solids in supersaturated conditions. Thus, solids may not be formed despite
370 being in supersaturated conditions unless nucleation and crystal growth favor precipitation conditions. The
371 kinetics of precipitation of each species can differ significantly, but nucleation and initial precipitation of
372 one solid can accelerate in cascade the rate of solid formation for all supersaturated species. As can be seen
373 in Figure 4d, simultaneous existence of non-carbonate hardness Ca^{2+}, Mg^{2+} and carbonate hardness during
374 the ERN might lead to formation of multiple solids. At pH >10.5 in water matrix *Ca^{2+}:CO_3^{2-}:Mg^{2+}* 1:1:0.25
375 at equilibrium state, the precipitation of solids such as $CaCO_{3(s)}$, $CaMg(CO_3)_{2(s)}$, and $Mg(OH)_{2(s)}$ is
376 thermodynamically favorable to occur.
377 Figure 5 evaluates the impact of co-existing CO_3^{2-} at the given initial Ca^{2+} concentration in the
378 ground water matrix of 1 mM Ca^{2+}. Increasing concentration of CO_3^{2-} decreases nitrate reduction, which
379 can be explained by the enhanced insolubility of Ca^{2+} species driven by the precipitation of $CaCO_3$. The
380 initial nitrate reduction of 74% observed in the simple quaternary brackish solution containing only Ca^{2+}
381 (Table 1 Entry D with *Ca^{2+}:CO_3^{2-}:Mg^{2+}* 1:0:0) is almost equivalent to the one obtained in the blank solution
382 without Ca^{2+} (Table 1 Entry A with 0:0:0). In contrast, the ERN performance decreased to 54% in the
383 presence of equimolar concentration of Ca^{2+} and CO_3^{2-} (1:1:0). It is important to note that solubility
384 diagrams describe the thermodynamic trend to precipitate in supersaturated conditions, but they do not

specify how fast the precipitation reaction will occur because if supersaturated conditions are reached, precipitation depends on kinetics of nucleation and crystal growth. Figure 5 illustrates also how a small content of Mg^{2+} of 0.25 mM (1:1:0.25) strongly impacted nitrate reduction performance by further decreasing nitrate removal to 35%. These results illustrate the relevance of synergistic effect of hardness ions, which induce electrode scaling and inhibit the ERN treatment.

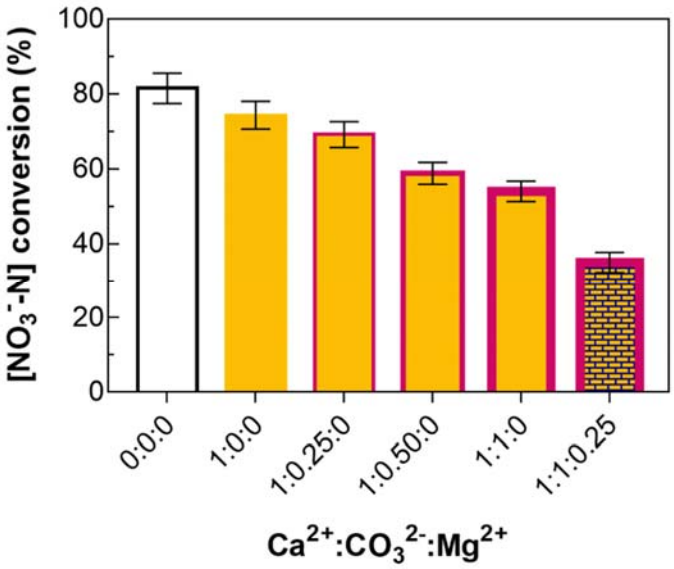

Figure 5. *Impact of coexisting calcium, carbonate, and magnesium ions on nitrate conversion after 360 min of ERN on Sn cathode at 40 mA* cm^{-2}*. The graph illustrates impact of different molar ratios* $Ca^{2+}:CO_3^{2-}:Mg^{2+}$ *for initial concentration of* Ca^{2+} *of 1 mM.*

X-ray fluorescence spectroscopy (XRF) is a non-destructive and fast surface analysis that provides information on elemental composition. XRF measurements provide a holistic view of the impact on the electrode surface of coexisting ions that might be associated to undesired scaling. When Sn electrodes (cathodes) were analyzed before electrolysis, the XRF only identified Sn as the solely elemental composition of pristine electrodes. Figure 6a shows the XRF analysis of the same cathodes after the treatment of pure nitrate solution (blank), the synthetic brackish groundwater, and solutions with individual cations, entries A, B, and C to E in Table 1, respectively. The XRF analysis did not detected calcium in any

402 case, but identified magnesium and silicon on the electrode surface after ERN for water samples described
403 in entries D and B. The quantification of these elements may suggest the incrustation of SiO_2 particles as
404 well as the precipitation of insoluble Mg^{2+} species. The treatment of nitrate in presence of solely silica salts
405 (entry E in Table 1) resulted in a lower quantity of Si detected, which may be justified by the role of Mg^{2+}
406 precipitate that form inorganic scaling on the electrode surface and might simultaneously co-precipitate
407 silica. Meanwhile, an increase in percentage of Mg on the surface was observed for solutions containing
408 solely nitrate and Mg^{2+} (entry D in Table 1).
409 The visually whitish solid formed on the cathode surface during the treatment of water sample
410 described in entry D was collected, dried at 60 °C, and analyzed by XRD. The diffractogram of Fig. 6b
411 shows the characteristic peaks of magnesium hydroxide with the hexagonal crystallographic structure of
412 brucite ($Mg(OH_2)$) (Donneys-Victoria et al., 2020; Pang et al., 2011). The crystallographic planes with
413 Miller indices of (001), (100), (101), (102), (110), (111), (103), and (201) were observed at 2θ angles of
414 18.3, 32.8, 37.9, 50.8, 58.6, 61.9, 68.2 and 72.0, respectively. The precipitation of brucite can be explained
415 by the high alkaline localized pH near the cathode surface that induces supersaturation conditions of Mg^{2+},
416 and therefore the nucleation of this insoluble species on the Sn cathode surface. The XRD analysis of the
417 whitish solid formed on the cathode after ERN of water sample described in entry B (synthetic brackish
418 groundwater) showed that besides brucite more complex inorganic salts were formed such as dolomite
419 ($CaMg(CO_3)_2$) and cristobalite (SiO_2). At the 2θ angle of 22, the crystallographic plane with Miller index
420 of (101) of tetragonal cristobalite was detected, and at the 2θ angle of 31.3, 33.2, 35.1, 41.6, 44.5, and 50.3
421 the crystallographic planes of hexagonal dolomite were observed with Miller indexes of (104), (006), (015),
422 (113), (202), and (018), respectively (Gregg et al., 2015; Jiang et al., 2012). These results confirmed that
423 the ERN inhibition in synthetic brackish groundwater is mainly associated to the electrode scaling due to
424 the precipitation of inorganic salts of Mg^{2+} and Ca^{2+}.
425

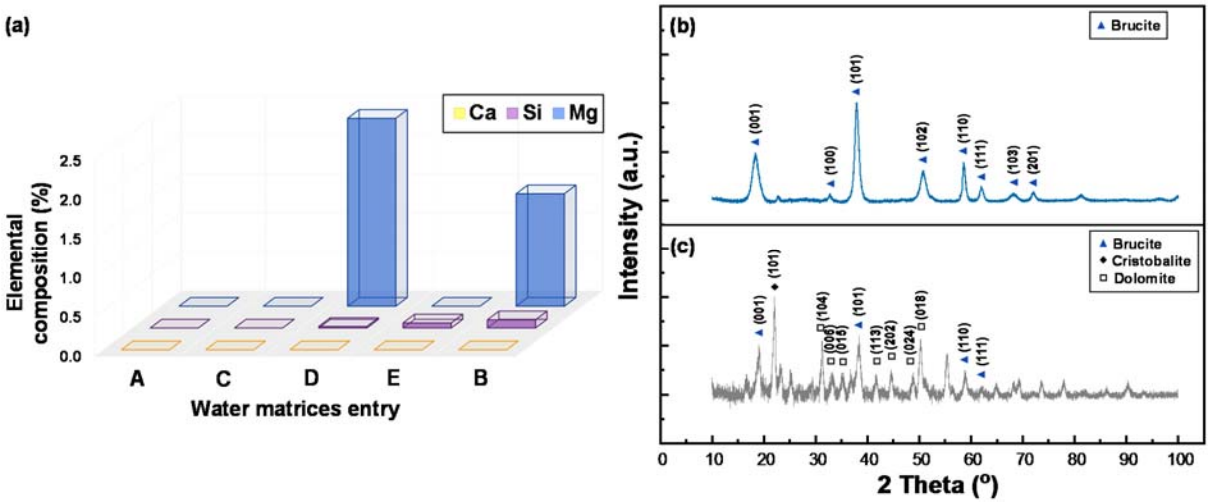

426

427 **Figure 6.** *(a) Elemental percentage composition of non-tin elements on the Sn cathode surface after*
428 *ERN on different water matrices detected by XRF. XRD diffractogram of solid incrustation collected from*
429 *the cathode surface after electrocatalytic treatment of (b) a water matrix containing* Mg^{2+} *(entry D in Table*
430 *1) and the (c) synthetic brackish groundwater (entry B in Table 1).*

431

432 *3.3 Understanding boundaries limiting ERN feasibility on real water matrices*

433 The selective reduction by physic-chemical means that transform nitrate to innocuous nitrogen gas
434 can be a game changer for environmental protection. The treatment of nitrate contaminated real brackish
435 groundwater (entry J in Table 1) and reverse osmosis brines collected from an inland desalination water
436 treatment plant (entry L in Table 1) allowed identifying major barriers that coincide with those reported in
437 the previous section for synthetic brackish groundwater treatment (entry B in Table 1). Figure 7 illustrates
438 how the high fraction of nitrate removal achieved in a simple ternary brackish nitrate solution (entry A in
439 Table 1) substantially decreased when the electrochemically-driven technology of advanced reduction was
440 applied in a real water matrix scenario. Understanding barriers to technology adoption is an essential
441 element for engineering research since this can provide guidelines for technology application and/or
442 contribute to design preemptive strategies.

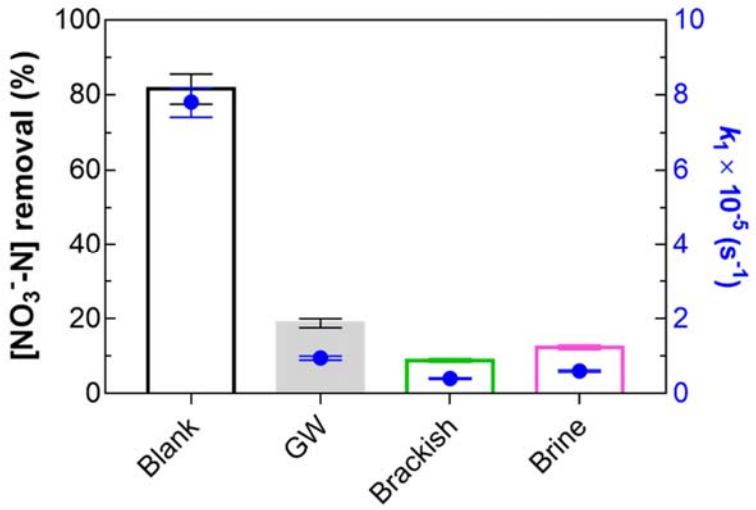

Figure 7. *Electrochemical nitrate removal (bars) and kinetic constants (full blue circles) of 30 mg NO_3^--N L^{-1} in a ternary brackish water (blank, entry A), a complex synthetic brackish groundwater (entry B), a real brackish groundwater (entry J), and RO brine (entry L) after 360 min of treatment at 40 mA cm^{-2}. Compositions are listed in Table 1.*

Similar to observations reported with the complex synthetic brackish groundwater, the Sn cathodes became scaled again with a white solid by treating real brackish groundwater and RO brine. The gel collected on the Sn cathode surface after the treatment using brine water (Figure 8a) was dried and analyzed by XRF, being identified mostly calcium, magnesium, and silicon as illustrated in Fig. 8b. The XRD diffractogram of the collected solid (see Figure 8c) had a predominant crystalline structure of calcite, which is the most stable polymorph insoluble $CaCO_3$ solid at alkaline pH (Guilheiro et al., 2021; Luo et al., 2020). Characteristic diffraction peaks at 2θ: 23.3, 29.6, 31.9, 36.1, 39.6, 43.3, 47.7, 48.7, 56.7, 57.5, 59.2, 60.8, 64.8, 65.7, 69.3, 70.4, 73.0, 77.3, 81.7 and 83.9 correspond to Miller Index planes of (012), (104), (006), (110), (113), (202), (018), (116), (211), (122), (208), (125), (300), (0012), (217), (0210), (128), (1112), (2110) and (134) that are associated with the hexagonal crystal system of calcite. The diffraction peaks at 18.6, 38.0, 50.9, and 58.7 related to the planes of (001), (011), (102), and (110) were characteristic signals

of brucite's hexagonal crystal system. The remaining peaks in the diffractogram corresponded to the hexagonal crystal system of dolomite observed at 22.1 and 45.0 with Miller Index planes of (101) and (202), respectively. These results highlight the relevant effect exerted by water hardness on scaling and the nature of the scalant formed.

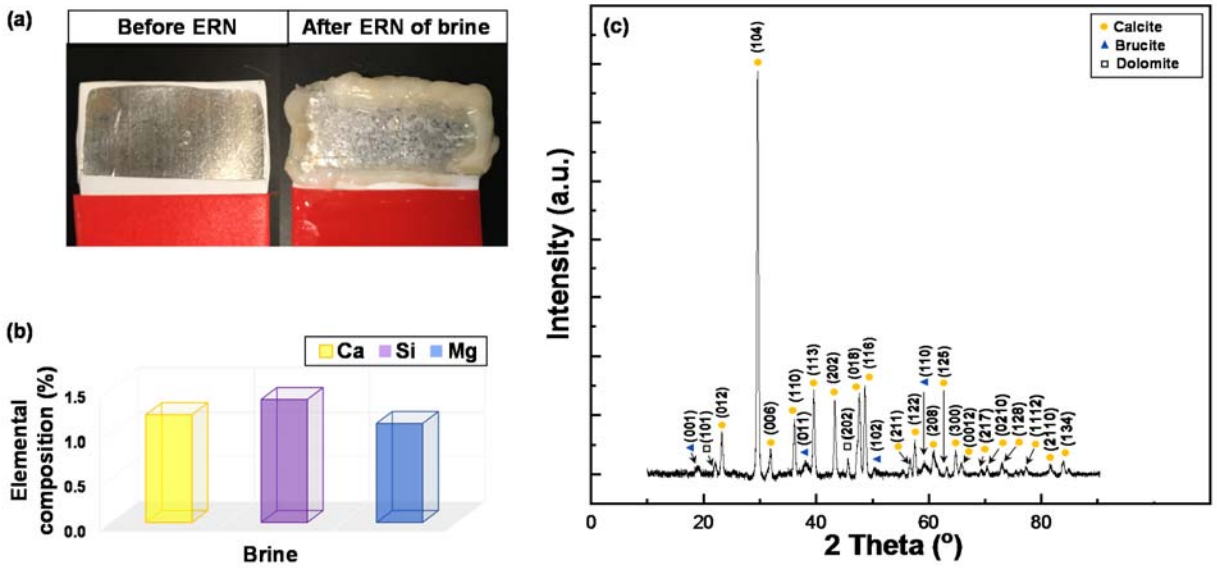

Figure 8. *Electrochemical reduction of nitrate treatment at 40 mA cm^{-2} in RO brine: (a) tin electrode before and after the electrolysis, (b) elemental composition of other elements different than tin on the Sn cathode surface after the electrolysis (tin corresponds to >98% of the XRF detected composition) and (c) XRD diffractogram of the solid incrustation collected from the cathode surface after treatment.*

Table 2. Summary of water hardness and alkalinity nature of representative water matrices and their effect on nitrate removal after 360 min of treatment at 40 mA cm^{-2} of 30 mg-N L^{-1} of nitrate by electrocatalytic reduction on tin cathodes.

Entry	Water Sample	Initial pH	Water hardness (meq L^{-1})	Hardness	$[Ca^{2+}]$ (mmol L^{-1})	$[Mg^{2+}]$ (mmol L^{-1})	$[HCO_3^-]$ (mmol L^{-1})	NO_3^- removal (%)
A	Blank	5.95	0	Very soft	0	0	0	75
I	Synthetic Brackish Groundwater	6.22	3.0	Hard	1.02	0.50	3.00	19
J	Real Brackish Groundwater	7.90	9.0	Very hard	3.24	1.23	1.62	9
K	Softened real brackish	10.5	2.1	Hard	n.m.	n.m.	n.m.	37
L	Real RO Brine	8.10	41.2	Very hard	14.1	6.46	6.84	12

Clearly, water hardness, and associated ions that adsorb to precipitated solids (e.g., silicates), are one of the major inhibitors of sustained ERN treatment. Table 2 suggests that the very hard characteristics of real brackish and RO brine waters may be indicative of high scaling risk and therefore the formation of a physical barrier on the electrode surface that will hamper the mass transport of nitrate from solution towards the electrocatalytic sites. Further consequences: 1) impermeable scale reduces electrode surface area, 2) semi-permeable scale causes an additional diffusion limited zone, and 3) scaling changes electrode interface and may induce electrostatic repulsion of nitrate ion. Understanding that the electrochemical reduction of water and nitrate induces a localized increase of pH on any electrocatalytic surface, water hardness can be identified as a major barrier for ERN treatment. Thereby, strategies that by-pass such shortcoming are considered herein.

A widely considered approach to mitigate scaling on electrodes is reverse polarization, but it is a strategy limited to electrodes that can sustain both anodic and cathodic polarization conditions without surface degradation or electrodissolution (Chow et al., 2021). It should be pointed out that some earth-abundant catalysts such as tin and copper may dissolve under anodic potentials (Fajardo et al., 2014; Speck and Cherevko, 2020), while some metal oxides commonly used in electrochemical water treatment (*e.g.,*

487 dimensional stable anodes) may suffer from cathodic corrosion and degrade under cathodic potentials. In
488 this frame, other approaches must be designed. Implementing a chemical or electrochemical pre-treatment
489 of water softening may be a feasible alternative to be explored (Sanjuán et al., 2019).
490
491 *3.4 Exploring benefits of water softening as pre-treatment to electrocatalysis*
492 Real brackish groundwater showed the highest inhibition of ERN (entry J in Table 2) with respect
493 to the idealistic conditions of ultrapure water solutions that are usually reported in research papers (entry A
494 in Table 2). Results suggest that the inhibiting effect is mostly associated with the scaling induced by water
495 hardness. Therefore, chemical softening was implemented as pre-treatment to evaluate if the decrease of
496 hardness cations and silica can reinstate ERN performance metrics. Figure 9 illustrates that decreasing
497 brackish water hardness from 9.0 meq L^{-1} down to 2.1 meq L^{-1} through lime soda ash softening positively
498 affects the electrocatalytic nitrate conversion (softened real brackish, entry K in Table 2). ERN attained 9%
499 nitrate conversion in real brackish groundwater after 360 min of electrocatalytic treatment with a 0.4×10^{-5}
500 s^{-1} kinetic rate constant for nitrate reduction (Figure 9a). Meanwhile, after softening real brackish
501 groundwater ERN achieved 37% nitrate conversion after 360 min of treatment (Figure 9b) with 5-fold
502 kinetics (k_1 of 2.1×10^{-5} s^{-1}). Visual inspection of the electrodes revealed a drastic difference since
503 appreciable scaling was not observed under softened water conditions. This effect was further verified
504 through XRF analyses that demonstrated a decrease in elemental composition of calcium and silicon on the
505 cathode (see Figure 9c); note that magnesium was not identified during XRF analyses of these samples.

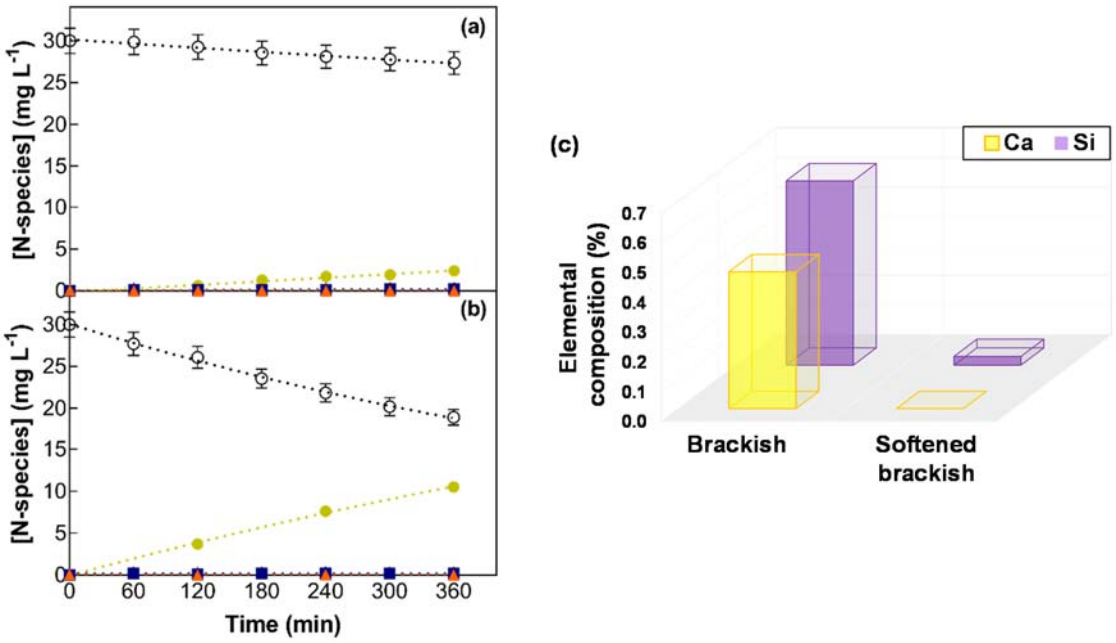

506 **Figure 9.** *Time course of nitrogenated species ((○) NO_3^--N, (▲) NO_2^--N, (■) NH_3-N, (●) N_2-N) over time*
507 *for the electrochemical reduction of 30 mg NO_3^--N L^{-1} at 40 mA cm^{-2} in (a) real brackish water with total*
508 *hardness of 9.0 meq L^{-1} and (b) softened real brackish water with total hardness of 2.1 meq L^{-1} as $CaCO_3$.*
509 *(c) Comparative elemental analysis by XRF of Sn electrode surface after ERN on real brackish and softened*
510 *real brackish groundwaters.*

511

512 The benefits of pre-softening brackish water were analyzed in function of engineering figures of
513 merit related to FE and EE/O. Figure 10 shows the detrimental effect of scaling formation on the cathode.
514 Scaling decreases charge transfer efficiency from a FE of 24 % in the blank (entry A in Table 2) down to a
515 discrete FE of 3 % for real brackish groundwater (entry J in Table 2). Meanwhile, negligible effect was
516 observed in terms of N_2 gas selectivity that maintained a similar value of ~95 ±2 % for brackish and softened
517 brackish water. However, the notorious decrease in FE showed an impact on the treatment economics.
518 Noteworthy is that EE/O drastically increases by 16-fold from 102 kWh m^{-3} $order^{-1}$ for the blank up to 1612
519 kWh m^{-3} $order^{-1}$ for the Brackish water. The increase in EE/O which can be explained by the decrease in
520 mass transfer of nitrate form solution towards the electrode surface because of the electrode scaling, but

521 also by the increased resistance induced by the physical barrier of the crystalized insoluble salts on the
522 cathode. Softening treatment can improve performance of ERN under real water matrix conditions and
523 effectively increase FE up to 13 % and diminish the EE/O down to 310 kWh m^{-3} $order^{-1}$ (entry K in Table
524 2). These results allow inferring the driving role of water hardness as a barrier for effective reduction of
525 nitrate in real water matrices. Implementing pre-treatments that decrease water hardness can enable
526 successful translation of ERN technologies to decrease nitrate levels below MCL under real water matrix
527 conditions.
528

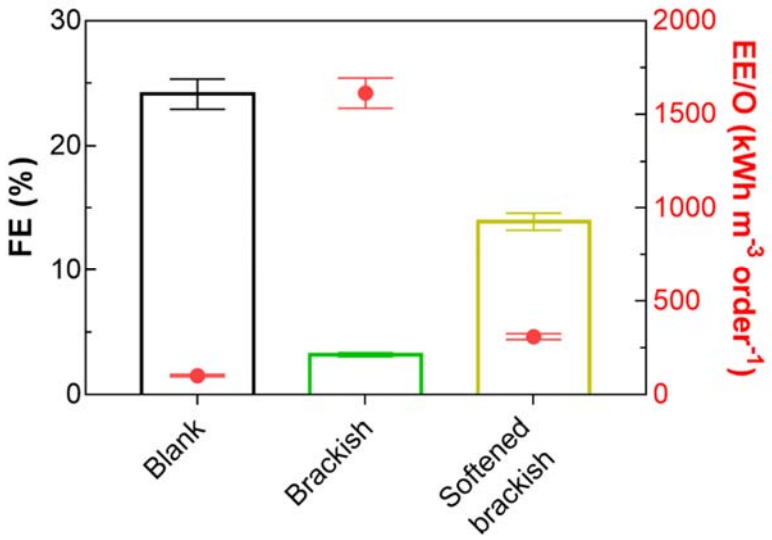

529 **Figure 10.** *Faradaic efficiency (bars) and electric energy per order (full red circles) after 360 min*
530 *of the ERN for the treatment of 30 mg* NO_3^-*-N* L^{-1} *at 40 mA* cm^{-2} *in simple ternary brackish, real brackish,*
531 *and softened real brackish waters (entries A, J and K in Table 2, respectively).*
532
533 In the United States, groundwaters commonly contain high nitrate concentrations, which impacts
534 both municipal and private groundwater wells. Private wells receive little attention and have no mandatory
535 treatments. In the USA alone there are ~45 million people that may be impacted by high nitrate
536 concentrations in water sources (EPA, 2017; Pennino et al., 2017). Human activities such as fertilizer use,
537 manure application, and sewage treatment can contaminate sources of drinking water with nitrate, which

can easily leach through soil into groundwater and surface water. The maps illustrated in Figure 11 show the comparative distribution of high nitrate concentration and the water hardness distribution around the US. It is important to remark that not all the areas experience simultaneously hard waters with high concentrations of nitrate. However, the South-West illustrates several overlapping water quality conditions that lead to high nitrate concentrations and high-water hardness, which may represent a barrier for electrochemical reduction of nitrate without conducting a preliminary softening. Thus, opportunities for commercialization lay ahead for these regions that require development of hybrid softening/nitrate removal systems. However, most regions that face high nitrate concentration in soft waters (see Figure 11) can still benefit from direct deployment of electrochemical point of use (POU) treatment units. Our research results demonstrate that strategies that minimize scaling will benefit implementation and adoption of emerging ERN technologies. Beyond chemical softening, other emerging research opportunities arise to design strategies to prevent scaling formation such as the use of current pulses, implementation of anion-exchange films to prevent water hardness ions transport close to the electrode surface, or surface modifications that may decrease scaling extent (e.g., hydrophobic vs hydrophilic surfaces, nanostructures, crystallographic interface engineering, etc.) (Garcia-Segura et al., 2020b; Hanssen et al., 2016).

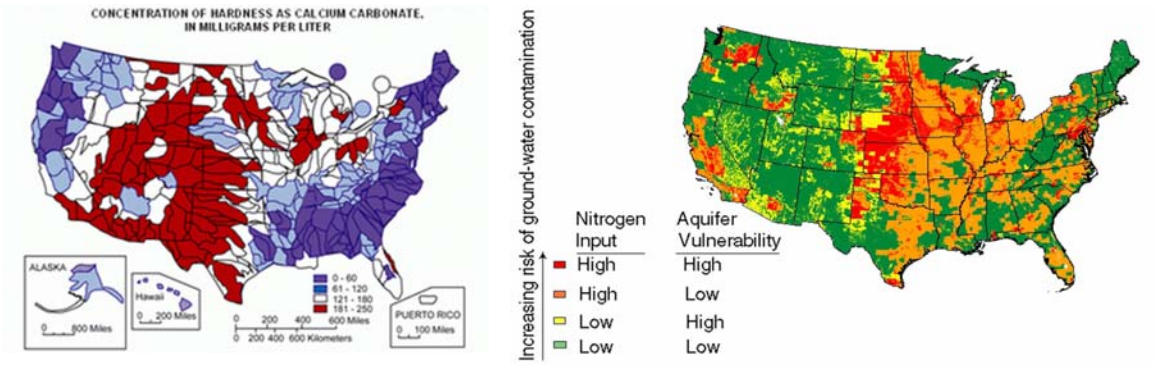

Figure 11. *Geographic information system mapping of (a) water hardness and (b) nitrogen input in USA* (USGS, 2018, 2005) .

559 **4. Conclusions**

560 This work explores in what extent the most common anions/cations present in natural water sources
561 (synthetic brackish groundwater, real brackish groundwater, and RO brine) affect the electrochemical
562 reduction of nitrate. The effect of controlling pH over time was analyzed showing that the maintenance of
563 circumneutral pH during the ERN of synthetic solution did not result in either an acceleration of kinetics
564 nor an increase in nitrogen gas selectivity. Therefore, the solution pH was not controlled in the following
565 electrochemical treatment experiments.

566 Electrochemical reduction of nitrate in a brackish groundwater matrix that contains a complex
567 mixture of coexisting ionic species showed a 4-fold decrease when compared against a conventional
568 synthetic solution (containing only sodium nitrate and sodium sulfate as electrolyte). The drastic loss in
569 performance was attributed to inorganic scaling formation on the cathode surface. Brucite ($Mg(OH)_2$),
570 calcite ($CaCO_3$) and dolomite ($CaMg(CO_3)_2$) compounds precipitated on the cathode surface during the
571 electrolysis. Silicon was also detected at the cathode, and likely adsorbed or co-precipitated with this water
572 hardness related minerals. Collectively, formation of these precipitates decreased the ERN efficiency by
573 creating a physical barrier, which makes difficult the electron transfer at the electrode surface.

574 The treatment of real brackish and brine waters (maximum nitrate conversion ~ 9 and 12%,
575 respectively) allowed to recognize key obstacles that match with those verified for the treatment of the
576 synthetic brackish groundwater. The perception of these barriers and their effect on the technology
577 translation are fundamental aspects to offer ideas for technology application and/or promote the outline of
578 new action plans. The Sn cathodes became scaled with a white solid for both real waters. The gel collected
579 on the surface of the cathode after treatment using brine water was analyzed by XRF that identified Ca^{2+},
580 Mg^{2+}, and SiO_2. These results emphasized the importance of the water hardness on scaling and the nature
581 of the scalant formed. Chemical water softening was used as a pre-treatment to assess if decreasing the
582 amount of Mg^{2+} and Ca^{2+} could improve the ERN performance. Softening pre-treatment enabled an increase
583 of 4-fold in the ERN, together with an acceleration in the reduction kinetics of 5-fold and a decrease of 5-
584 fold in the electric energy per order (EE/O). During this treatment no visual scaling was observed on the

surface of the Sn electrode. Understanding that in the US most of the regions with high risk of groundwater contamination by nitrate overlap with areas with high water hardness, makes it clear that there is a need for water softening pre-treatment prior ERN implementation. The results presented in this manuscript outline research opportunities to enhance sustained performance of ERN treatments by developing compatible preemptive anti-scaling strategies (e.g., current pulses, implementation of anion-exchange, or cathode engineering).

Acknowledgments

This material is based upon research supported by the Transatlantic Research Partnership of the Embassy of France in the United States and the FACE Foundation. This project has received funding from the European Union's Horizon 2020 research and innovation program under the Marie Sklodowska-Curie grant agreement No 843870. This work was partially funded by the National Science Foundation (NSF) through the Nanosystems Engineering Research Center for Nanotechnology-Enabled Water Treatment under project EEC-1449500. The authors acknowledge the support of the Centre National de la Recherche Scientifique (CNRS). We thank De Nora Tech, LLC for kindly providing the DSA® electrodes used as anode in our electrochemical system. The use of facilities within the Eyring Materials Center at Arizona State University supported in part by NNCI-ECCS-1542160 is acknowledged.

603 **References**

604 Abdelfattah, A., Hossain, M.I., Cheng, L., 2020. High-strength wastewater treatment using microbial
605 biofilm reactor: a critical review. World J. Microbiol. Biotechnol. 36, 1–10.
606 https://doi.org/10.1007/s11274-020-02853-y

607 Allaire, M., Wu, H., Lall, U., 2018. National trends in drinking water quality violations. Proc. Natl. Acad.
608 Sci. U. S. A. 115, 2078–2083. https://doi.org/10.1073/pnas.1719805115

609 Ambrosioni, B., Barthelemy, A., Bejan, D., Bunce, N.J., 2014. Electrochemical reduction of aqueous nitrate
610 ion at tin cathodes. Can. J. Chem. 92, 228–233. https://doi.org/10.1139/cjc-2013-0406

611 Amma, L.V., Ashraf, F., 2020. Brine Management in Reverse Osmosis, in: 2020 Advances in Science and
612 Engineering Technology International Conferences.

613 Bolton, J.R., Bircher, K.G., Tumas, W., Tolman, C.A., 2001. Figures-of-merit for the technical
614 development and application of advanced oxidation technologies for both electric- and solar-driven
615 systems (IUPAC Technical Report). Pure Appl. Chem. 73, 627–637.
616 https://doi.org/10.1351/pac200173040627

617 Cerrón-Calle, G. A., Fajardo, A.S., Sánchez-Sánchez, C.M., Garcia-Segura, S., 2022. Highly reactive Cu-
618 Pt bimetallic 3D-electrocatalyst for selective nitrate reduction to ammonia. Appl. Catal. B Environ.
619 302, 120844. https://doi.org/10.1016/j.apcatb.2021.120844

620 Cerrón-Calle, G.A., Magdaleno, A.L., Graf, J.C., Apul, O.G., Garcia-Segura, S., 2022a. Elucidating CO2
621 nanobubble interfacial reactivity and impacts on water chemistry. J. Colloid Interface Sci. 607, 720–
622 728. https://doi.org/10.1016/j.jcis.2021.09.033

623 Cerrón-Calle, G.A., Senftle, T.P., Garcia-Segura, S., 2022b. Strategic tailored design of electrocatalysts for
624 environmental remediation based on density functional theory (DFT) and microkinetic modelling.
625 Curr. Opin. Electrochem. 35, 101062.

626 Chao, P., Westerhoff, P., 2002. Assessment and optimization of chemical and physicochemical softening
627 processes. J. Am. Water Work. Assoc. 94, 109–119.

628 Chaplin, B.P., 2019. The prospect of electrochemical technologies advancing worldwide water treatment.

629 Acc. Chem. Res. 52, 596–604. https://doi.org/10.1021/acs.accounts.8b00611
630 Chow, H., Ingelsson, M., Roberts, E.P.L., Pham, A.L.T., 2021. How does periodic polarity reversal affect
631 the faradaic efficiency and electrode fouling during iron electrocoagulation? Water Res. 203, 117497.
632 https://doi.org/10.1016/j.watres.2021.117497
633 Crittenden, J.C., Trussel, R.R., Hand, D.W., Howe, K.J., Tchobanoglous, G., 2012. Water treatment
634 principles and design, 3rd ed. Wiley, New Jersey.
635 Donneys-Victoria, D., Marriaga-Cabrales, N., Machuca-Martínez, F., Benavides-Guerrero, J., Cloutier,
636 S.G., 2020. Indigo carmine and chloride ions removal by electrocoagulation. Simultaneous production
637 of brucite and layered double hydroxides. J. Water Process Eng. 33, 101106.
638 https://doi.org/10.1016/j.jwpe.2019.101106
639 Dortsiou, M., Katsounaros, I., Polatides, C., Kyriacou, G., 2013. Influence of the electrode and the pH on
640 the rate and the product distribution of the electrochemical removal of nitrate. Environ. Technol.
641 (United Kingdom) 34, 373–381. https://doi.org/10.1080/09593330.2012.696722
642 dos Santos, A.J., Fajardo, A.S., Kronka, M.S., Garcia-Segura, S., Lanza, M.R.V., 2021. Effect of
643 electrochemically-driven technologies on the treatment of endocrine disruptors in synthetic and real
644 urban wastewater. Electrochim. Acta 376, 138034. https://doi.org/10.1016/j.electacta.2021.138034
645 EPA, 2017. Estimated nitrate concentrations in groundwater used for drinking.
646 Fajardo, A.S., Martins, R.C., Quinta-Ferreira, R.M., 2014. Treatment of a synthetic phenolic mixture by
647 electrocoagulation using Al, Cu, Fe, Pb, and Zn as anode materials. Ind. Eng. Chem. Res. 53, 18339–
648 18345. https://doi.org/10.1021/ie502575d
649 Fajardo, A.S., Westerhoff, P., Sanchez-Sanchez, C.M., Garcia-Segura, S., 2021. Earth-abundant elements
650 a sustainable solution for electrocatalytic reduction of nitrate. Appl. Catal. B Environ. 281, 119465.
651 https://doi.org/10.1016/j.apcatb.2020.119465
652 Flores, K., Antonio, G., Valdes, C., Atrashkevich, A., Castillo, A., Morales, H., Parsons, J.G., Garcia-
653 segura, S., Gardea-torresdey, J.L., 2022. Outlining Key Perspectives for the Advancement of
654 Electrocatalytic Remediation of Nitrate from Polluted Waters. ACS ES&T Eng. 2, 746–768.

655 https://doi.org/10.1021/acsestengg.2c00052
656 Fuladpanjeh□Hojaghan, B., Elsutohy, M.M., Kabanov, V., Heyne, B., Trifkovic, M., Roberts, E.P.L., 2019.
657 In□Operando Mapping of pH Distribution in Electrochemical Processes. Angew. Chemie 131,
658 16971–16975. https://doi.org/10.1002/ange.201909238
659 Garcia-Segura, S., Arotiba, O.A., Brillas, E., 2021. The pathway towards photoelectrocatalytic water
660 disinfection: Review and prospects of a powerful sustainable tool. Catalysts 11, 1–29.
661 https://doi.org/10.3390/catal11080921
662 Garcia-Segura, Sergi, Lanzarini-Lopes, M., Hristovski, K., Westerhoff, P., 2018. Electrocatalytic reduction
663 of nitrate: Fundamentals to full-scale water treatment applications. Appl. Catal. B Environ. 236, 546–
664 568. https://doi.org/10.1016/j.apcatb.2018.05.041
665 Garcia-Segura, S., Lanzarini-Lopes, M., Hristovski, K., Westerhoff, P., 2018. Electrocatalytic reduction of
666 nitrate: Fundamentals to full-scale water treatment applications. Appl. Catal. B Environ. 236.
667 https://doi.org/10.1016/j.apcatb.2018.05.041
668 Garcia-Segura, S., Nienhauser, A.B., Fajardo, A.S., Bansal, R., Coonrod, C.L., Fortner, J.D., Marcos-
669 hernández, M., Rogers, T., Villagran, D., Wong, M.S., Westerhoff, P., 2020a. Disparities between
670 Experimental and Environmental Conditions : Research Steps Towards Making Electrochemical
671 Water Treatment. Curr. Opin. Electrochem. 22, 9–16. https://doi.org/10.1016/j.coelec.2020.03.001
672 Garcia-Segura, S., Qu, X., Alvarez, P.J.J., Chaplin, B.P., Chen, W., Crittenden, J.C., Feng, Y., Gao, G., He,
673 Z., Hou, C.H., Hu, X., Jiang, G., Kim, J.H., Li, J., Li, Q., Ma, Jie, Ma, Jinxing, Nienhauser, A.B., Niu,
674 J., Pan, B., Quan, X., Ronzani, F., Villagran, D., Waite, T.D., Walker, W.S., Wang, C., Wong, M.S.,
675 Westerhoff, P., 2020b. Opportunities for nanotechnology to enhance electrochemical treatment of
676 pollutants in potable water and industrial wastewater-a perspective. Environ. Sci. Nano 7, 2178–2194.
677 https://doi.org/10.1039/d0en00194e
678 Gregg, J.M., Bish, D.L., Kaczmarek, S.E., Machel, H.G., 2015. Mineralogy, nucleation and growth of
679 dolomite in the laboratory and sedimentary environment: A review. Sedimentology 62, 1749–1769.
680 https://doi.org/10.1111/sed.12202

Gröhlich, A., Langer, M., Mitrakas, M., Zouboulis, A., Katsoyiannis, I., Ernst, M., 2017. Effect of organic matter on Cr(VI) removal from groundwaters by Fe(II) reductive precipitation for groundwater treatment. Water (Switzerland) 9, 389. https://doi.org/10.3390/w9060389

Guilheiro, J.M., Tatumi, S.H., Soares, A. de F., Courrol, L.C., Barbosa, R.F., Rocca, R.R., 2021. Correlation study between OSL, TL and PL emissions of yellow calcite. J. Lumin. 233, 117881. https://doi.org/10.1016/j.jlumin.2020.117881

Hansen, B., Thorling, L., Schullehner, J., Termansen, M., Dalgaard, T., 2017. Groundwater nitrate response to sustainable nitrogen management. Sci. Rep. 7, 1–12. https://doi.org/10.1038/s41598-017-07147-2

Hanssen, B.L., Siraj, S., Wong, D.K.Y., 2016. Recent strategies to minimise fouling in electrochemical detection systems. Rev. Anal. Chem. 35, 1–28. https://doi.org/10.1515/revac-2015-0008

Jiang, X., Bao, L., Cheng, Y.S., Dunphy, D.R., Li, X., Brinker, C.J., 2012. Aerosol-assisted synthesis of monodisperse single-crystalline α-cristobalite nanospheres. Chem. Commun. 48, 1293–1295. https://doi.org/10.1039/c1cc15713b

Katsounaros, I., 2021. On the assessment of electrocatalysts for nitrate reduction. Curr. Opin. Electrochem. 28, 100721. https://doi.org/10.1016/j.coelec.2021.100721

Katsounaros, I., Dortsiou, M., Kyriacou, G., 2009. Electrochemical reduction of nitrate and nitrite in simulated liquid nuclear wastes. J. Hazard. Mater. 171, 323–327. https://doi.org/10.1016/j.jhazmat.2009.06.005

Katsounaros, I., Dortsiou, M., Polatides, C., Preston, S., Kypraios, T., Kyriacou, G., 2012. Reaction pathways in the electrochemical reduction of nitrate on tin. Electrochim. Acta 71, 270–276. https://doi.org/10.1016/j.electacta.2012.03.154

Katsounaros, I., Kyriacou, G., 2008. Influence of nitrate concentration on its electrochemical reduction on tin cathode: Identification of reaction intermediates. Electrochim. Acta 53, 5477–5484. https://doi.org/10.1016/j.electacta.2008.03.018

Lertratwattana, K., Kemacheevakul, P., Garcia-Segura, S., Lu, M.C., 2019. Recovery of copper salts by fluidized-bed homogeneous granulation process: High selectivity on malachite crystallization.

Hydrometallurgy 186, 66–72. https://doi.org/10.1016/j.hydromet.2019.03.015

Li, P., Karunanidhi, D., Subramani, T., Srinivasamoorthy, K., 2021. Sources and Consequences of Groundwater Contamination. Arch. Environ. Contam. Toxicol. 80, 1–10. https://doi.org/10.1007/s00244-020-00805-z

Lim, J., Liu, C.Y., Park, J., Liu, Y.H., Senftle, T.P., Lee, S.W., Hatzell, M.C., 2021. Structure Sensitivity of Pd Facets for Enhanced Electrochemical Nitrate Reduction to Ammonia. ACS Catal. 11, 7568–7577. https://doi.org/10.1021/acscatal.1c01413

Liu, Z., Haddad, M., Sauvé, S., Barbeau, B., 2021. Alleviating the burden of ion exchange brine in water treatment: From operational strategies to brine management. Water Res. 205, 117728. https://doi.org/10.1016/j.watres.2021.117728

Luo, X., Song, X., Cao, Y., Song, L., Bu, X., 2020. Investigation of calcium carbonate synthesized by steamed ammonia liquid waste without use of additives. RSC Adv. 10, 7976–7986. https://doi.org/10.1039/c9ra10460g

Marcos-Hernández, M., Antonio Cerrón-Calle, G., Ge, Y., Garcia-Segura, S., Sánchez-Sánchez, C.M., Fajardo, A.S., Villagrán, D., 2022. Effect of surface functionalization of Fe3O4 nano-enabled electrodes on the electrochemical reduction of nitrate. Sep. Purif. Technol. 282, 119771. https://doi.org/10.1016/j.seppur.2021.119771

Martínez-Huitle, C.A., Brillas, E., 2021. A critical review over the electrochemical disinfection of bacteria in synthetic and real wastewaters using a boron-doped diamond anode. Curr. Opin. Solid State Mater. Sci. 25, 100926. https://doi.org/10.1016/j.cossms.2021.100926

Martínez-Huitle, C.A., Rodrigo, M.A., Sirés, I., Scialdone, O., 2015. Single and Coupled Electrochemical Processes and Reactors for the Abatement of Organic Water Pollutants: A Critical Review. Chem. Rev. 115, 13362–13407. https://doi.org/10.1021/acs.chemrev.5b00361

Maxwell, B., Díaz-García, C., Martínez-Sánchez, J.J., Álvarez-Rogel, J., 2020. Increased brine concentration increases nitrate reduction rates in batch woodchip bioreactors treating brine from desalination. Desalination 495, 114629. https://doi.org/10.1016/j.desal.2020.114629

733 Monteiro, M.C.O., Koper, M.T.M., 2021. Measuring local pH in electrochemistry. Curr. Opin.
734 Electrochem. 25, 100649. https://doi.org/10.1016/j.coelec.2020.100649
735 Moreira, F.C., Boaventura, R.A.R., Brillas, E., Vilar, V.J.P., 2017. Electrochemical advanced oxidation
736 processes: A review on their application to synthetic and real wastewaters. Appl. Catal. B Environ.
737 202, 217–261. https://doi.org/10.1016/j.apcatb.2016.08.037
738 Nobial, M., Devos, O., Mattos, O.R., Tribollet, B., 2007. The nitrate reduction process: A way for
739 increasing interfacial pH. J. Electroanal. Chem. 600, 87–94.
740 https://doi.org/10.1016/j.jelechem.2006.03.003
741 Pang, H., Ning, G., Gong, W., Ye, J., Lin, Y., 2011. Direct synthesis of hexagonal Mg(OH)2 nanoplates
742 from natural brucite without dissolution procedure. Chem. Commun. 47, 6317–6319.
743 https://doi.org/10.1039/c1cc10279f
744 Pennino, M.J., Compton, J.E., Leibowitz, S.G., 2017. Trends in Drinking Water Nitrate Violations Across
745 the United States. Environ. Sci. Technol. 51, 13450–13460. https://doi.org/10.1021/acs.est.7b04269
746 Rupert, M.G., 2008. Decadal-scale changes of nitrate in ground water of the United States, 1988-2004. J.
747 Environ. Qual. 37, S240–S248. https://doi.org/10.2134/jeq2007.0055
748 Sanjuán, I., Benavente, D., Expósito, E., Montiel, V., 2019. Electrochemical water softening: Influence of
749 water composition on the precipitation behaviour. Sep. Purif. Technol. 211, 857–865.
750 https://doi.org/10.1016/j.seppur.2018.10.044
751 Sanjuán, I., García-Cruz, L., Solla-Gullón, J., Expósito, E., Montiel, V., 2020. Bi–Sn nanoparticles for
752 electrochemical denitrification: activity and selectivity towards N2 formation. Electrochim. Acta 340.
753 https://doi.org/10.1016/j.electacta.2020.135914
754 Snoeyink, V.L., Jenkins, D., 1980. Water Chemistry. John Wiley & Sons, Inc., New York.
755 Speck, F.D., Cherevko, S., 2020. Electrochemical copper dissolution: A benchmark for stable CO2
756 reduction on copper electrocatalysts. Electrochem. commun. 115, 106739.
757 https://doi.org/10.1016/j.elecom.2020.106739
758 Su, L., Li, K., Zhang, H., Fan, M., Ying, D., Sun, T., Wang, Y., Jia, J., 2017. Electrochemical nitrate

759 reduction by using a novel Co3O4/Ti cathode. Water Res. 120, 1–11.
760 https://doi.org/10.1016/j.watres.2017.04.069
761 Szpyrkowicz, L., Daniele, S., Radaelli, M., Specchia, S., 2006. Removal of NO3- from water by
762 electrochemical reduction in different reactor configurations. Appl. Catal. B Environ. 66, 40–50.
763 https://doi.org/10.1016/j.apcatb.2006.02.020
764 Tada, K., Shimazu, K., 2005. Kinetic studies of reduction of nitrate ions at Sn-modified Pt electrodes using
765 a quartz crystal microbalance. J. Electroanal. Chem. 577, 303–309.
766 https://doi.org/10.1016/j.jelechem.2004.11.039
767 Temkin, A., Evans, S., Manidis, T., Campbell, C., Naidenko, O. V., 2019. Exposure-based assessment and
768 economic valuation of adverse birth outcomes and cancer risk due to nitrate in United States drinking
769 water. Environ. Res. 176, 108442. https://doi.org/10.1016/j.envres.2019.04.009
770 Tlili, M.M., Benamor, M., Gabrielli, C., Perrot, H., Tribollet, B., 2003. Influence of the Interfacial pH on
771 Electrochemical CaCO[sub 3] Precipitation. J. Electrochem. Soc. 150, C765.
772 https://doi.org/10.1149/1.1613294
773 Torres, E.G., Morales, R.P., Zamora, A.G., Sánchez, E.R., Calderón, E.H.O., Romero, J. de J.A., Rincón,
774 E.Y.C., 2020. Consumption of water contaminated by nitrate and its deleterious effects on the human
775 thyroid gland: a review and update. Int. J. Environ. Health Res. 00, 1–18.
776 https://doi.org/10.1080/09603123.2020.1815664
777 USGS, 2018. Nitrogen and Water [WWW Document]. URL https://www.usgs.gov/special-topics/water-
778 science-school/science/nitrogen-and-water
779 USGS, 2005. Map of water hardness in the United States [WWW Document]. URL
780 https://www.usgs.gov/media/images/map-water-hardness-united-states
781 Usman, M., Katsoyiannis, I., Mitrakas, M., Zouboulis, A., Ernst, M., 2018. Performance evaluation of small
782 sized powdered ferric hydroxide as arsenic adsorbent. Water (Switzerland) 10, 957.
783 https://doi.org/10.3390/w10070957
784 van Langevelde, P.H., Katsounaros, I., Koper, M.T.M., 2021. Electrocatalytic nitrate reduction for

785 sustainable ammonia production. Joule 5, 290–294. https://doi.org/10.1016/j.joule.2020.12.025
786 Villanueva-Rodríguez, M., Sánchez-Sánchez, C.M., Montiel, V., Brillas, E., Peralta-Hernández, J.M.,
787 Hernández-Ramírez, A., 2012. Characterization of ferrate ion electrogeneration in acidic media by
788 voltammetry and scanning electrochemical microscopy. Assessment of its reactivity on 2,4-
789 dichlorophenoxyacetic acid degradation. Electrochim. Acta 64, 196–204.
790 https://doi.org/10.1016/j.electacta.2012.01.021
791 Werth, C.J., Yan, C., Troutman, J.P., 2021. Factors Impeding Replacement of Ion Exchange with
792 (Electro)Catalytic Treatment for Nitrate Removal from Drinking Water. ACS ES&T Eng. 1, 6–20.
793 https://doi.org/10.1021/acsestengg.0c00076
794 WHO, 2016. Nitrate and nitrite in drinking-water [WWW Document].
795 Yang, T., Doudrick, K., Westerhoff, P., 2013. Photocatalytic reduction of nitrate using titanium dioxide for
796 regeneration of ion exchange brine. Water Res. 47, 1299–1307.
797 https://doi.org/10.1016/j.watres.2012.11.047
798 Zhang, X., Wang, Y., Liu, C., Yu, Y., Lu, S., Zhang, B., 2021. Recent advances in non-noble metal
799 electrocatalysts for nitrate reduction. Chem. Eng. J. 403, 126269.
800 https://doi.org/10.1016/j.cej.2020.126269
801 Zhang, Y., Mahdavi, B., Mohammadhosseini, M., Rezaei-Seresht, E., Paydarfard, S., Qorbani, M.,
802 Karimian, M., Abbasi, N., Ghaneialvar, H., Karimi, E., 2021. Green synthesis of NiO nanoparticles
803 using Calendula officinalis extract: Chemical charactrization, antioxidant, cytotoxicity, and anti-
804 esophageal carcinoma properties. Arab. J. Chem. 14, 103105.
805 https://doi.org/10.1016/j.arabjc.2021.103105
806